Hindawi
Journal of Computer Networks and Communications
Volume 2019, Article ID 5149529, 7 pages
https://doi.org/10.1155/2019/5149529

Research Article

Design of Rhombus-Shaped Slot Patch Antenna for Wireless Communications

Manavalan Saravanan and Madihally Janardhana Srinivasa Rangachar

Department of Electronics and Communication Engineering, Hindustan Institute of Technology and Science, Chennai, India

Correspondence should be addressed to Manavalan Saravanan; msarawins@gmail.com

Received 23 August 2018; Accepted 29 October 2018; Published 10 January 2019

Academic Editor: Rui Zhang

A single feed circularly polarized patch antenna is presented. The antenna consists of a rhombus-shaped slot incorporated in the radiating patch at its center. The antenna is designed to operate at 2.3 GHz band. The antenna achieves left-hand polarization or right-hand polarization based on the orientation of the slot in the radiating patch. The antenna parameters are synthesized using a high-frequency structure simulator and its characteristics are validated by the Agilent network analyzer (N9925A) and antenna test systems. The measured results obtained agree with simulated results and show that the antenna achieves −10 dB impedance bandwidth of 85 MHz (2.27 GHz–2.355 GHz) for left-hand polarization and 85 MHz (2.26 GHz–2.345 GHz) for right-hand polarization. The antenna gives a 3 dB axial ratio beamwidth of 95°(−35° ≤ AR ≤ 60°) for both left-hand polarization and right-hand polarization along with better 3 dB axial ratio bandwidth of 140° in the operating band. The antenna also achieves a good cross-polarization isolation of −17 dBic for both left-hand and right-hand polarization at its operating frequency. Hence, the antenna is best suited for modern wireless communication systems.

1. Introduction

Compact circular polarized patch antennas play a vital role in satellite communications and airborne communication due to their low profile and lightweight. These antennas require low cross-polarization isolation in order to mitigate multipath interference and wider axial ratio beamwidth to provide a wide coverage area. However, 3 dB axial ratio beamwidth of the antenna suffers from a narrow beamwidth and cannot meet the required practical applications. A lot of researchers have been proposed to improve axial ratio beamwidth and to reduce cross-polarization isolation. One way of improving the beamwidth is to employ a 3D ground structure as in [1, 2]. These structures utilize a multilayer stacked structure which diffracts the electromagnetic waves from the ground plane, thereby altering the radiation pattern of the antenna. However, these structures increase the overall width of the antenna. In [3], the beamwidth of the antenna is improved by altering the spacing between the two crossed dipoles placed in a square-shaped contour. However, it results in a bidirectional radiation pattern and thus results in power loss in the undesired direction. Another way of improving the beamwidth is by exciting surface waves through substrates extended on the ground plane as given in [4]. This technique significantly produces backward radiations, thereby interfering with other circuit elements.

A popular technique to improve the beamwidth is by introducing parasitic elements around the patch. However, the space required for these patch elements are higher and hence increases the overall length of the antenna [5]. A 3D circularly polarized patch is presented in [6]. The antenna uses a crossed slot in the radiating patch, and a triangular feed structure is made to improve the bandwidth of the antenna. Though the techniques discussed increase the axial ratio beamwidth of the antenna, the technique fails to suppress the cross-polarization isolation, especially at low elevation angles [7, 8]. One more technique to improve the beamwidth is by introducing lumped elements in the radiating patch. In [9], PIN diodes are placed along diagonals

of the square patch, and the beamwidth is fully controlled by the shunt inductive load. The antenna uses the dual feed to excite two orthogonal modes. In [10, 11], a circularly polarized antenna with an improved axial ratio beamwidth is proved. However, it suffers from poor cross-polarization isolation. In [12], parasitic stubs are used to perturb the surface fields on the radiating patch to achieve circular polarization with an improved axial ratio beamwidth. Recently, a slot of appropriate shape is etched in the circular radiating patch is used to achieve circular polarization [13–15].

In this paper, a rhombus-shaped slot patch antenna operating at 2.3 GHz band is presented. The antenna is fabricated on FR4 substrate, and its performance is measured using the Agilent network analyzer and antenna test systems. The measured results are compared with simulation results and show that the antenna is best suited for airborne wireless communication systems.

2. Geometry of Proposed Antenna

The geometry of the proposed antenna is illustrated in Figure 1. The antenna is fabricated on fire retardant dielectric substrate (FR4) having a relative permittivity of $\varepsilon_r = 4.4$ and dielectric loss tangent of $\zeta = 0.02$. In order to have low profile thickness, the substrate is chosen to have a thickness of 1.6 mm. A rhombus-shaped slot is etched in the radiating element in order to excite two orthogonal modes. This perturbs the surface current over the patch element, thereby generating circular polarization. The orientation of the slot determines the nature of polarization. The antenna is fed by 50 Ω SMA connector. A quarter wave transformer having an impedance of 50 Ω is used for impedance matching.

2.1. Surface Current Distribution. The surface current distribution over the radiating patch is simulated and is shown in Figure 2. Figure 2(a) shows surface current distribution corresponding to left-hand circular polarization (LHCP). Here, surface current in the right half plane along X-axis perturbs near the corner of the slot in advance when compared to the left half plane. This adds a 90° phase delay in the surface current between both the half planes, which results in LHCP. Figure 2(b) shows surface current distribution corresponds to right-hand circularly polarization (RHCP). Here, surface current in the left half plane along X-axis perturbs near the corner of the slot in advance when compared to the right half plane. This adds a 90° phase delay in the surface current between both the half planes, which results in LHCP. Thus, based on the orientation of the slot, the antenna achieves either left-hand or right-hand polarization.

3. Antenna Design Considerations

A circular shape is considered as the basic antenna geometry shape for the proposed antenna model. Hence, the radius of the circular patch [16] is calculated from the following equation:

$$a = \frac{1.8412 * c}{2\pi * f_r * \sqrt{\varepsilon_r}}, \quad (1)$$

where a = radius of the patch (m), c = velocity of light in vacuum = $3 * 10^8$ m/s, f_r = resonant frequency (GHz), and ε_r = relative permittivity = 4.4 (no unit).

The introduction of the slot in the radiating element increases the electrical length of the antenna and it shifts the operating frequency. Therefore, an offset length introduced in the radial length of the patch is needed and is given in the following equation:

$$R = a - \left(0.0134 * \frac{\lambda}{\sqrt{\varepsilon_r}}\right), \quad (2)$$

where R = effective radius of the antenna.

Since slot dimensions greatly affect the purity of polarization, the dimension of the slot has to be carefully chosen for the antenna to radiate circular polarization. The following equation gives optimal slot dimension of the proposed model:

$$L = \frac{R}{4.7},$$
$$\text{Slot}_X = \sqrt{2L}, \quad (3)$$
$$\text{Slot}_Y = \frac{3}{2}L.$$

Table 1 gives overall dimensions of the proposed antenna model operating at the 2.3 GHz band.

4. Results and Discussions

To verify the feasibility of the presented circular polarized antenna, a prototype is fabricated on FR_4 substrate having a thickness of 1.6 mm. A 50 Ω SMA connector is used to feed the model.

In order to analyze the characteristics of the proposed antenna, the prototype is tested using the network analyzer N9924A as shown in Figure 3, and its radiation characteristics are measured using the antenna test setup shown in Figure 4. A 50 Ω N-type adapter is used to couple the network analyzer with the model.

The impedance curve measured using a network analyzer is shown in Figure 5 and is compared with simulation results. It is observed that the antenna resonates at 2.3 GHz band and achieves a −10 dB impedance bandwidth of 85 MHz (2.27 GHz–2.355 GHz) for left-hand polarization and 85 MHz (2.26 GHz–2.345 GHz) for right-hand polarization. In order to validate the radiation characteristics, the fabricated model is tested under the antenna test system. The measured radiation characteristics are compared with simulation results and are shown in Figure 6.

A standard pyramidal horn antenna having a gain of 9 dB is used as a reference antenna. The distance between two antennas (R) is measured, and the gain is calculated using the Friis transmission equation given below:

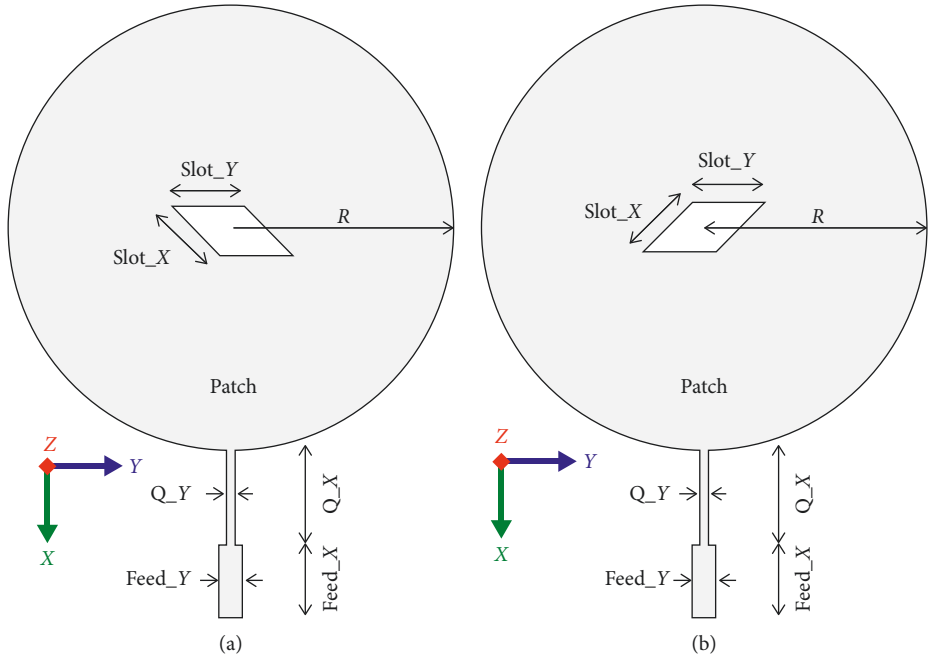

Figure 1: Antenna geometry. (a) LHCP. (b) RHCP.

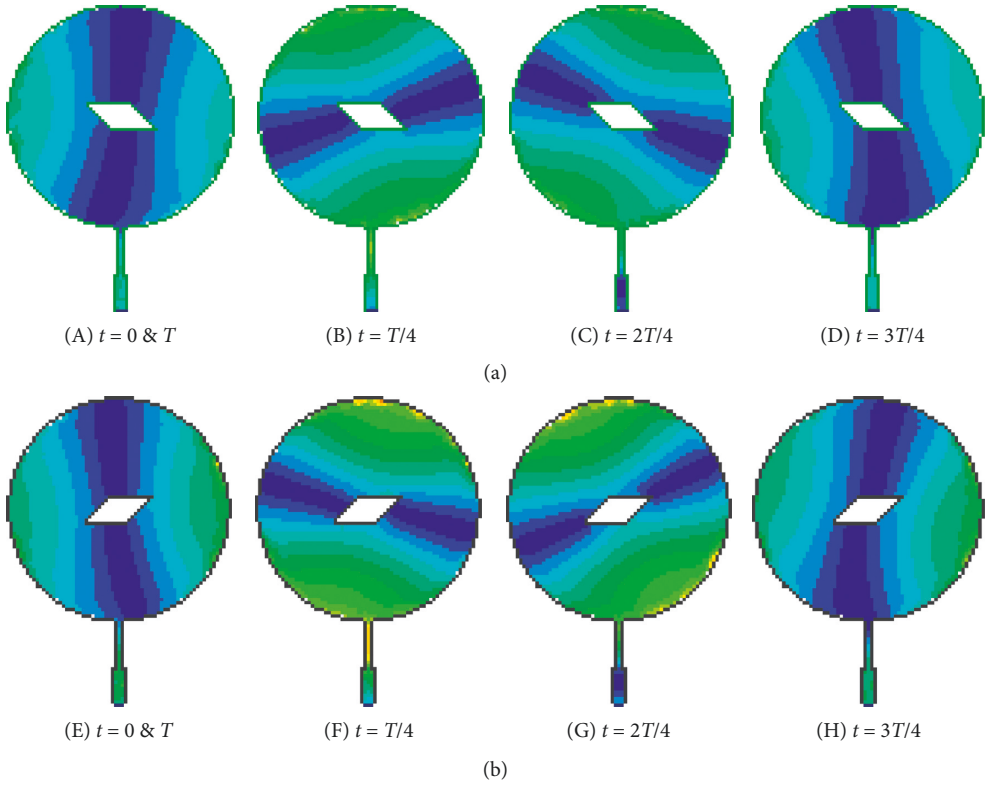

Figure 2: Simulated surface current distribution. (a) LHCP. (b) RHCP.

$$\frac{P_r}{P_t} = \left(\frac{\lambda}{4\pi R}\right)^2 G_t G_r. \quad (4)$$

Figure 6(a) shows measured radiation characteristics corresponding to antenna geometry shown in Figures 1(a) and 6(b) and measured radiation characteristics corresponding to antenna geometry shown in Figure 1(b). The simulation results agree with measured results, and the antenna gives symmetrical radiation pattern around zenith. The antenna achieves a good cross-polarization isolation of

Table 1: Antenna design specifications.

Parameters	Specifications
Operating frequency	2.3 GHz
R	17.39 mm
L	3.70 mm
Slot_X ∗ Slot_Y	5.23 mm ∗ 5.55 mm
Q_X ∗ Q_Y	12 mm ∗ 0.96 mm
Feed_X ∗ Feed_Y	8 mm ∗ 2.4 mm

Figure 3: Testing of antenna.

Figure 4: Radiation pattern measurement setup.

−17 dBic for both LHCP and RHCP configurations at its operating frequency.

Figure 7 shows a variation of axial ratio against frequencies for both LHCP and RHCP configurations. It is observed from Figure 7 that the antenna gives minimum axial ratio at the 2.3 GHz operating frequency for both the configurations and achieves a measured wide 3 dB axial ratio bandwidth of 140 MHz in the operating band.

Figure 8 shows measured E plane and H plane radiation characteristics of both LHCP and RHCP configurations. It is observed that the antenna achieves a good axial ratio (AR)

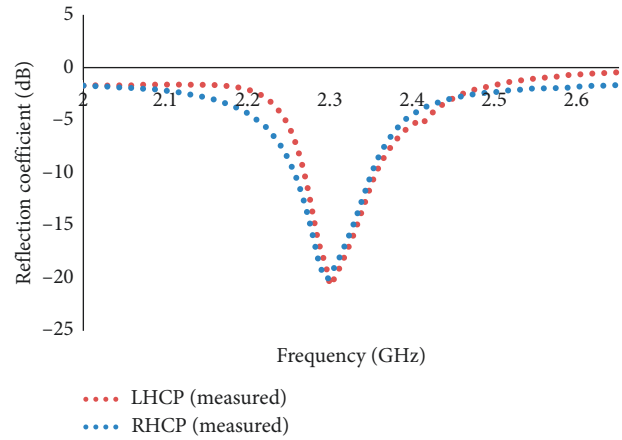

Figure 5: Reflection coefficient (dB).

over a wide beam angle ratio beamwidth of 95°(−35° ≤ AR ≤ 60°) for left-hand polarization and 95°(−35° ≤ AR ≤ 60°) for right-hand polarization. The measured gain is calculated using the gain comparison method. A standard pyramidal horn antenna having a gain of 9 dB is used as a reference antenna as shown in Figure 4. The distance between two antennas (R) is measured, and the gain is calculated using Friis transmission equation.

The gain characteristics of the proposed antenna with respect to operating band are given in Figure 9. It is observed that the antenna gives a nearly flat gain over the operating band. The measured gain for LHCP is 5.16 dBic and RHCP is 4.82 dBic at the boresight of the antenna. This small difference in gain results is due to fabrication loss and antenna alignment losses.

Table 2 gives performance comparison of proposed antenna with traditional antenna models. It is observed that the proposed model achieves better axial ratio bandwidth when compared to the traditional antenna model given in Table 2. Moreover, the cross-polarization isolation is better in the proposed antenna and is not studied in conventional antennas given in Table 2. In addition to this, the proposed antenna is simple and is modelled on the single layer instead of multilayer substrate as in Ref. [14], which makes it easy to integrate with other high-frequency circuits. Though the antenna has limitation of narrow 3 dB axial ratio bandwidth when compared to other traditional antennas, the 3 dB axial ratio beamwidth achieved by the proposed antenna is sufficient to cover one complete sector of a mobile cell network and also suitable for many wireless applications including MIMO application.

5. Conclusion

This paper introduces a novel circularly polarized patch antenna operating at 2.3 GHz. A rhombus-shaped slot is etched in radiating patch located at its center. The dimension of the slot is tuned to achieve minimum axial ratio at its operating frequency. The antenna radiates either left-hand or right-hand polarization based on the orientation of the slot. The measured radiation characteristics show that the proposed antenna attains 5.16 dBic for LHCP and 4.82 dBic

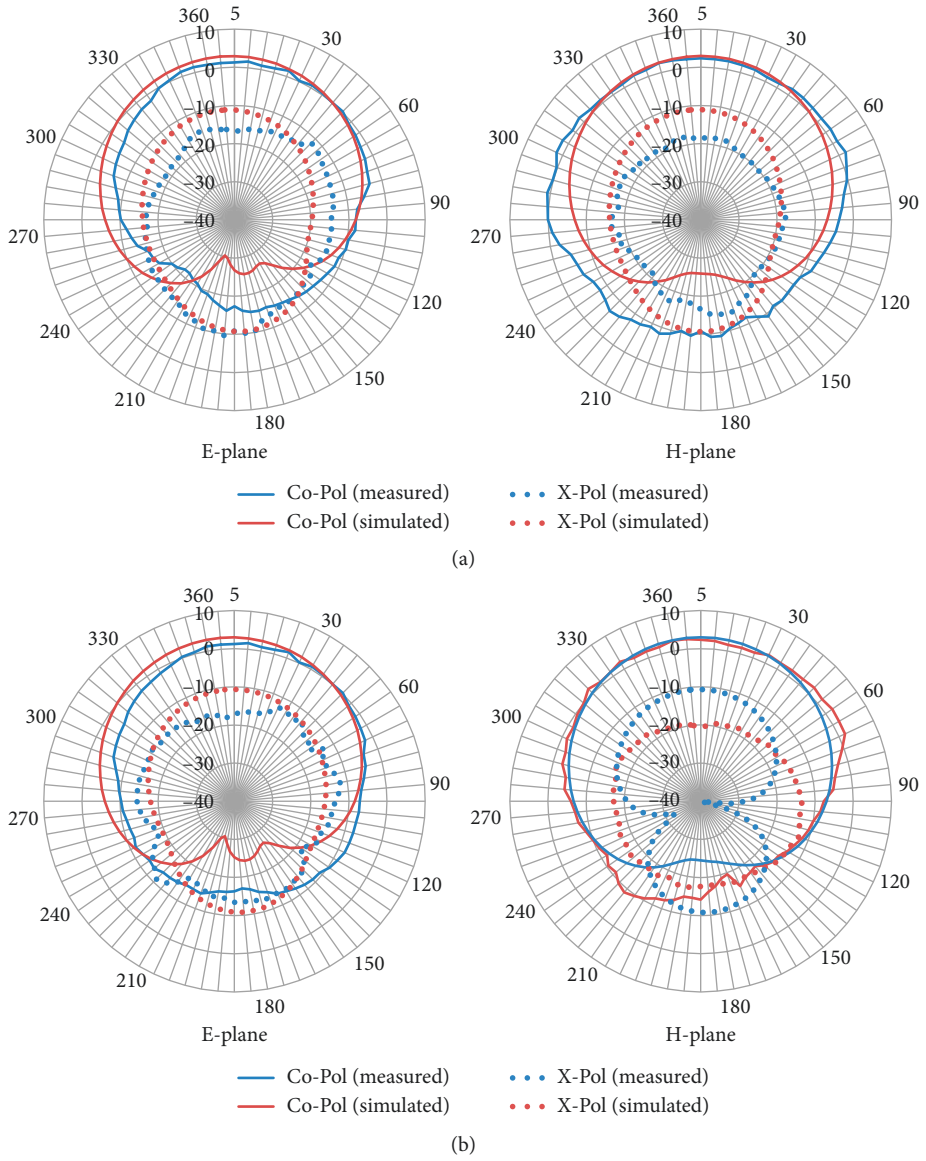

Figure 6: Simulated and measured radiation pattern of (a) LHCP and (b) RHCP.

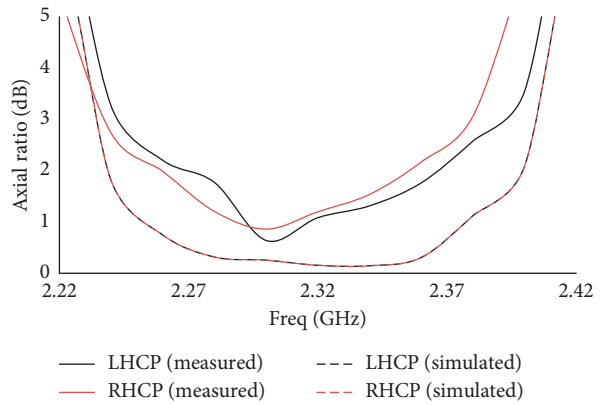

Figure 7: Axial ratio vs. frequency.

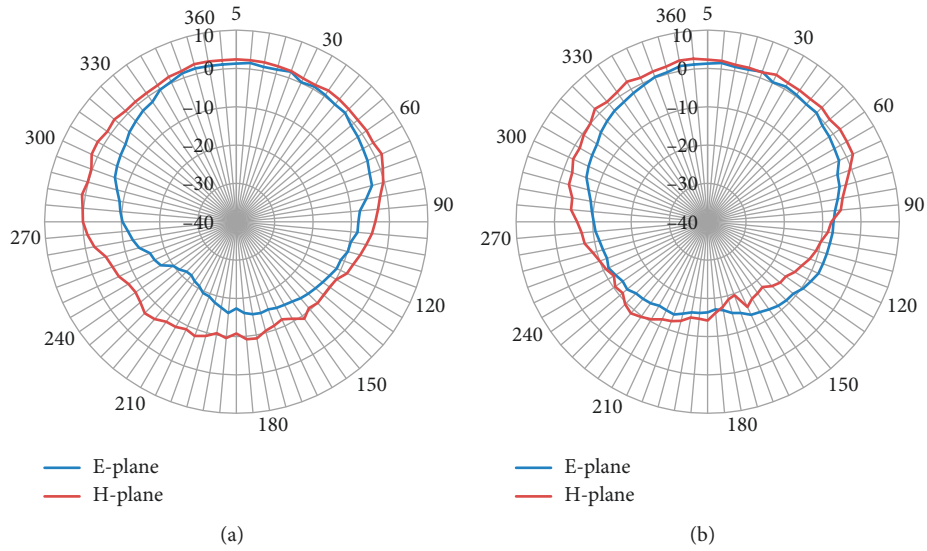

Figure 8: Radiation pattern measured at the minimum axial ratio. (a) LHCP. (b) RHCP.

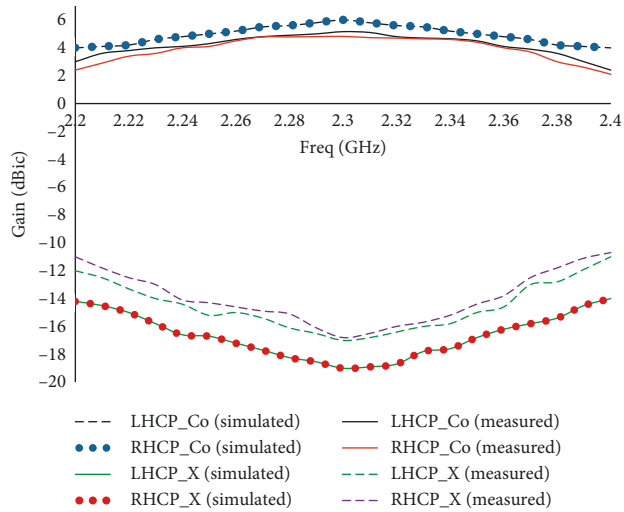

Figure 9: Variation of frequency (GHz) with respect to gain (dB).

Table 2: Performance comparison of the proposed model with the traditional antenna model.

Parameter	Ref. [12]	Ref. [13]	Ref. [14]	Ref. [15]	Proposed model
Reflection coefficient (dB)	−21 dB	−13 dB	−20 dB	−25 dB	−20.6 dB
Maximum gain (dB)	4.5 dB	5.3 dBic	6.8 dBic	6.1 dBic	5.16 dBic (LHCP) 4.82 dBic (RHCP)
3 dB axial ratio bandwidth (dB)	55 MHz	40 MHz	100 MHz	40 MHz	140 MHz
3 dB axial ratio beamwidth (dB)	176°	140°	100°	180°	95°
Cross-polarization isolation (dB)	NA	NA	NA	NA	−17 dB

for RHCP at the boresight of the antenna. The antenna achieves good cross-polarization isolation of −17 dBic and wider 3 dB axial ratio beamwidth of 95°(−35° ≤ AR ≤ 60°) for both left-hand polarization and right-hand polarization at operating frequency along with better 3 dB axial ratio bandwidth of 140° in the operating band which best suited for airborne communication.

Data Availability

No data were used to support this study.

Conflicts of Interest

The authors declare that they have no conflicts of interest.

References

[1] C.-L. Tang, J.-Y. Chiou, and K.-L. Wong, "Beamwidth enhancement of a circularly polarized microstrip antenna mounted on a three-dimensional ground structure," *Microwave and Optical Technology Letters*, vol. 32, no. 2, pp. 149–153, 2001.

[2] H. Jiang, Z. Xue, W. Li, and W. Ren, "Broad beamwidth stacked patch antenna with wide circularly polarised bandwidth," *Electronics Letters*, vol. 51, no. 1, pp. 10–12, 2015.

[3] Y. Luo, Q.-X. Chu, and L. Zhu, "A low-profile wide-beamwidth circularly-polarized antenna via two pairs of parallel dipoles in a square contour," *IEEE Transactions on Antennas and Propagation*, vol. 63, no. 3, pp. 931–936, 2015.

[4] N.-W. Liu, W.-W. Choi, and L. Zhu, "Low-profile wide-beamwidth circularly-polarised patch antenna on a suspended substrate," *IET Microwaves, Antennas and Propagation*, vol. 10, no. 8, pp. 885–890, 2016.

[5] K. Ding, C. Gao, D. Qu, and Q. Yin, "Compact broadband circularly polarized antenna with parasitic patches," *IEEE Transactions on Antennas and Propagation*, vol. 65, no. 9, pp. 4854–4857, 2017.

[6] X. Chen, Z. Wei, D. Wu, L. Yang, and G. Fu, "Low-cost and compact 3D circularly polarized microstrip antenna with high efficiency and wide beamwidth," *International Journal of Microwave and Wireless Technologies*, vol. 9, no. 7, pp. 1–8, 2017.

[7] X. Chen, L. Yang, J.-y. Zhao, and G. Fu, "High-Efficiency compact circularly polarized microstrip antenna with wide beamwidth for airborne communication," *IEEE Antennas and Wireless Propagation Letters*, vol. 15, pp. 1518–1521, 2016.

[8] J.-H. Lu and H.-S. Huang, "Planar compact dual-band monopole antenna with circular polarization for WLAN applications," *International Journal of Microwave and Wireless Technologies*, vol. 8, no. 1, pp. 81–87, 2014.

[9] X. Zhang, L. Zhu, and N.-W. Liu, "Pin-loaded circularly-polarized patch antennas with wide 3-dB axial ratio beamwidth," *IEEE Transactions on Antennas and Propagation*, vol. 65, no. 2, pp. 521–528, 2017.

[10] K. M. Mak and K. M. Luk, "A circularly polarized antenna with wide axial ratio beamwidth," *IEEE Transactions on Antennas and Propagation*, vol. 57, no. 10, pp. 3309–3312, 2009.

[11] G. Massie, M. Caillet, M. Clenet, and Y. M. M. Antar, "A new wideband circularly polarized hybrid dielectric resonator antenna," *IEEE Antennas and Wireless Propagation Letters*, vol. 9, pp. 347–350, 2010.

[12] S. B. Vignesh, N. Nasimuddin, and A. Alphones, "Stubs-integrated-microstrip antenna design for wide coverage of circularly polarised radiation," *IET Microwaves, Antennas and Propagation*, vol. 11, no. 4, pp. 444–449, 2017.

[13] L. B. K. Bernard, Nasimuddin, and A. Alphones, "AN e-shaped slotted-circular-patch antenna for circularly polarized radiation and radiofrequency energy harvesting," *Microwave and Optical Technology Letters*, vol. 58, no. 4, pp. 868–875, 2016.

[14] L. B. K. Bernard, Nasimuddin, and A. Alphones, "Teo-shaped slotted-circular-patch antenna for circularly polarized radiation and RF energy harvesting," *Microwave and Optical Technology Letters*, vol. 57, no. 12, pp. 2752–2758, 2015.

[15] A. M. Jie, Nasimuddin, M. F. Karim, L. Bin, F. Chin, and M. Ong, "A proximity-coupled circularly polarized slotted-circular patch antenna for RF energy harvesting applications," in *Proceedings of 2016 IEEE Region 10 Conference (TENCON)*, pp. 2027–2030, Jeju Island, Korea, November 2016.

[16] C. A. Balanis, *Antenna Theory: Analysis and Design*, Wiley-Interscience, Hoboken, NJ, USA, 3rd edition, 2005.